



OPEN

Optimization of salinity and composition of injected low salinity water into sandstone reservoirs with minimum scale deposition

Masoud Bijani¹, Ehsan Khamsehchi¹✉ & Mehdi Shabani²

In this study, a mechanistic and comprehensive examination of the impact of the scale formation situation of different diluted seawater levels was conducted to investigate the influence of important factors on the performance and efficiency of low salinity water. To clarify the effective participating mechanisms, scale precipitation by compatibility test, field emission scanning electron microscopy (FESEM) and energy dispersive X-ray spectroscopy (EDX) analysis, zeta potentials as surface charge, ion concentration changes, contact angle, pH, CO₂ concentration, electrical conductivity, and ionic strength were analyzed. The results showed that increasing the dilution time to the optimal level (10 times-diluted seawater (SW#10D)) could effectively reduce the amount of severe precipitation of calcium carbonate (CaCO₃) and calcium sulfate (CaSO₄) scales. However, the reduction in CaCO₃ scale precipitation (due to mixing different time diluted seawater with formation brine) and its effect on the wettability alteration (due to the change in surface charge of OLSW/oil and sandstone/OLSW) had higher impacts. The zeta potential results have shown that OLSW with optimum salinity, dilution, and ionic composition compared to different low salinity water compositions could change the surface charge of OLSW/oil/rock (– 16.7 mV) and OLSW/rock (– 10.5 mV) interfaces toward an extra negatively charged. FESEM and contact angle findings confirmed zeta potential results, i.e. OLSW was able to make sandstone surface more negative with diluting seawater and wettability changes from oil-wet toward water-wet. As a result, SW#10D was characterized by minimum scaling tendency and scale deposition (60 mg/l), maximum surface charge of OLSW/oil/rock (– 16.7 mV), and the potential of incremental oil recovery due to wettability alteration toward more water-wetness (the oil/rock contact angle ~ 50.13°) compared with other diluted seawater levels.

Fossil fuels are a significant portion of the worldwide energy supply¹. One of the oldest and well-known methods used in oil reservoirs for pressure maintenance and improved oil recovery is water injection. Water injection is the most considerably applied increased oil recovery method after the natural recovery of oil reservoirs². Lately, low salinity water injection (LSWI) and smart water injection (SWI) showed positive effects in the recovery factor of oil reservoirs³. Various laboratory experiments and field applications have shown increasing oil production because of modification of ion amount or reducing salinity level of seawater and increasing the dilution ratio of seawater^{4–11}. LSWI and SWI can be applied as improved oil production methods after changing the wettability of oil reservoirs^{12–16}. The prominent mechanisms of LSW flooding were wettability alteration, fine migration, rock dissolution, multiple ion exchange (MIE), and double layer expansion^{17,18}. Though, the dominant mechanism is referenced as wettability alteration in literature^{14,18}. Smart water as a kind of injection water can have two meanings under different definitions as follows^{19–21}:

- Application of saline water at low concentrations, neglecting the type of ions.
- Synthesis of a new water composition according to ion design considering their concentration and type.

¹Department of Petroleum Engineering, Amirkabir University of Technology (Tehran Polytechnic), Tehran, Iran. ²Regional Technical Advisor at STRATUM Reservoir, Middle East, Abu Dhabi, UAE. ✉email: Khamsehchi@aut.ac.ir

In this method, the amount of salinity decreases from about 1000 to 7000 ppm. Also, the potential determinant ions (PDI) of calcium (Ca^{2+}), magnesium (Mg^{2+}), and sulfate (SO_4^{2-}) in injection water change the wettability of rock towards higher hydrophilicity and increase oil recovery^{14,22–26}. Divalent ions include calcium (Ca^{2+}), magnesium (Mg^{2+}), and sulfate (SO_4^{2-}) activate surface charges. Also their concentrations in the solution determine the polarity and surface charge density of the rock and affects the reaction between oil and the rock surface²⁷. According to results obtained from the tertiary water injection method in oil reservoirs, 18% incremental oil recovery was obtained by diluted seawater in a stepwise manner, 2, 10, and 20-times diluted seawater. Subsequently, the two leading causes during smart water flooding can modify the wetting characteristics of sandstone and carbonate rocks as wettability alteration as follow^{12,14,28,29}:

1. Increased divalent ion concentrations (including Ca^{2+} , Mg^{2+} , and SO_4^{2-}) in the injected seawater.
2. Reduced salinity of the injected brine.

Thus, according to previous studies that modifying the composition of injected brine can result in more oil produced from oil reservoirs. Injection brine composition is a more important factor in scale deposition because scale formation happens when the formation water is mixed with other incompatible brines such as injected waters³⁰. Formation water has high-level salinity, total dissolved solids (TDS), total suspended solids (TSS), and different anions and cations in solution³¹. It indicates that the composition of the injected seawater is a significant quantitative parameter also the injected seawater quality should control similarly. It is important to examine the compatibility of smart water and low salinity water with reservoir conditions to prevent the scale formation³². Briefly, the possibility of the mineral scale formation as formation damage in oil reservoirs during smart water and low salinity water is important because of incompatible waters when mixing the brine injection with the formation water. To date, various studies have been conducted to evaluate the incompatibility of formation water and injection water³³. Two major types of inorganic scales that are usually formed in oil reservoirs during water flooding operations are sulfate and carbonate scales^{34,35}. One of the main causes of carbonate scales is usually the incompatibility of formation and injection waters mixing with different ratios of calcium and bicarbonate-rich water like seawater mixed with formation water. It can precipitate calcium carbonate and iron carbonate^{35,36}. Calcium carbonate (CaCO_3) as an inorganic scale in calcite form can contribute to difficult oil industry problems. Therefore, scale formation inhibition is more useful than the removal of scales and the use of inhibitors in different chemicals and solvents. These operations are economically costly and contribute to environmental problems³⁷. Predicting the potential scaling is one of the most effective methods for controlling the risk of problems such as scale formation during water flooding operations³⁸. This would be pretty helpful for handling mineral scale challenges and developing the most effective technique for inhibiting the formation of scales in oil fields³⁶. The present study was conducted to explore the most critical challenges of water-flooding process associated with the potential of mineral scale deposition like CaCO_3 during the experiment of low-salinity water flooding in a sandstone reservoir. Few researches have been done on accurate investigation of important factors on scale precipitation of injected brines during low salinity water injection for EOR in oil reservoirs. Unlike previous experimental works^{3,12,13,39–45}, the present study set to extend the investigation of scale formation in different low salinity water compositions by different effective parameters together. These parameters include the effect of salinity, dilution ratios of seawater, electrical conductivity (EC), ionic strength (IS) of brines, type and concentration of ions and salts, pH, and surface charge in aqueous solution on scale formation and wettability alteration.

The objectives of the study were as following:

1. Examining the effects of ions (Ca^{2+} , HCO_3^- , and Mg^{2+}), the salinity of injection brines, physicochemical parameters such as pH, EC, IS, CO_2 concentration as solution in brine. In addition, dilution times of seawater on the amount of CaCO_3 precipitation from mixing seawater, diluted seawater levels, and formation water with Ca^{2+} ions were investigated.
2. Optimizing the ion contents and diluted seawater levels as low salinity water to improve wettability alteration and reduce the formation damage.
3. Evaluating the effect of optimum LSW composition with minimum scale precipitation on wettability alteration.
4. Assessing the compatibility of thermodynamic data obtained from the mixed brines using OLI ScaleChem and comparing the collected data and experimental results.

An analysis of effective parameters was conducted in this research. To achieve objective 1, we investigated the type and amount of scale deposition by water compatibility experiments, pH, ionic strength, electrical conductivity measurements, and FESEM-EDX experiments. To achieve objectives 2 and 3, the effect of different low salinity water compositions and optimum low salinity water on wettability alteration were investigated by contact angle tests, FESEM, and the brine/rock and brine/oil surfaces charges by zeta potential experiments. Finally, to achieve objective 4, OLI ScaleChem software, brine compatibility experiments, and FESEM-EDX experiments were used to match experimental data and simulation also the results were compared together. Figure 1 shows a schematic diagram of the simulation and experiment steps for all scenarios. While Fig. 1A shows steps of preparation of thin sections and rock powders and after aging rock samples process in the reservoir conditions. Also, Fig. 1B shows steps of investigation of important factors on scale formation during compatibility experiments of injected brines with formation water. Finally, Fig. 1C presents steps of selection of optimum low salinity water composition and identifying the dominate mechanisms.

This research opens new horizons in compatibility experiments for optimization of dilution ratio and ion composition of LSW injection technique for EOR with minimum scale risk and high wettability change performance,

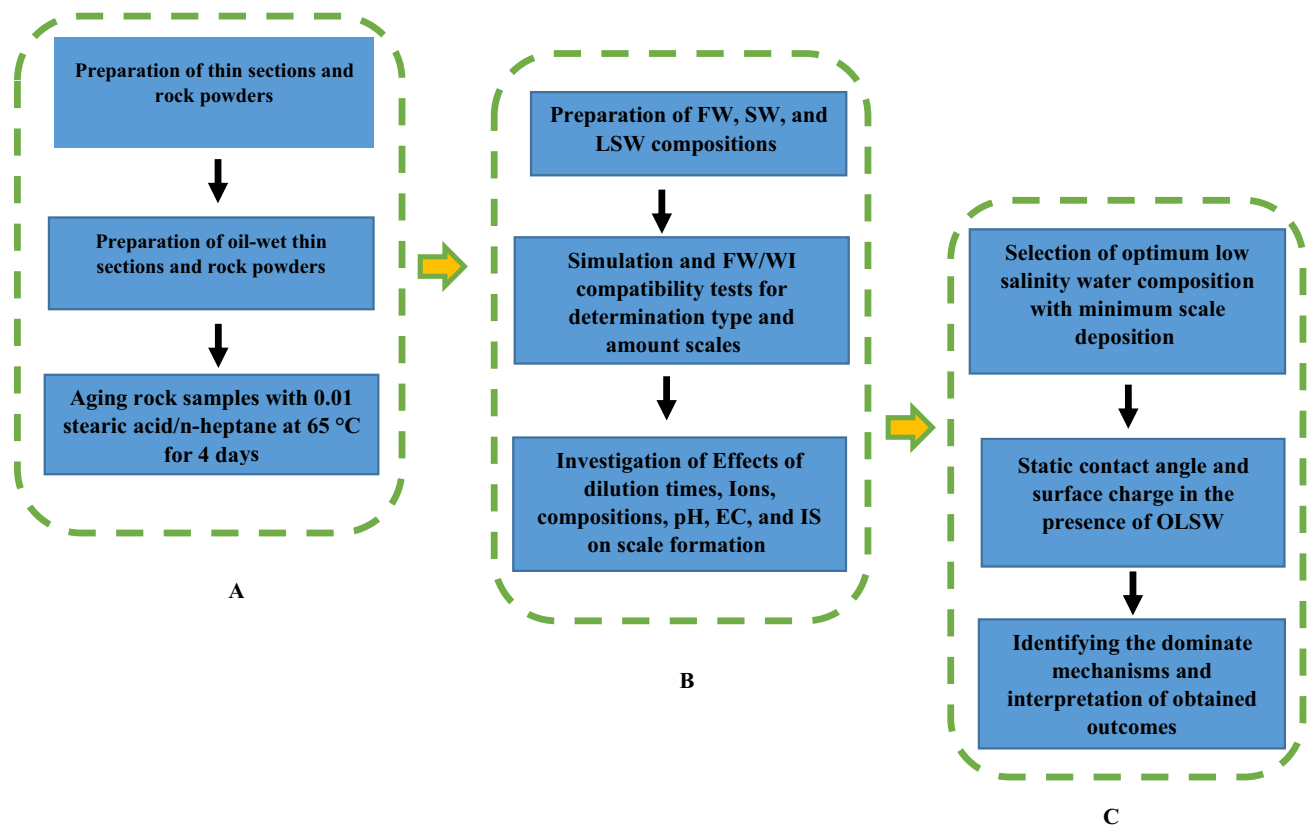


Figure 1. Schematic diagram of the experiment and simulation steps.

which has not been investigated before. Also, this research has the novel points as following: (1) unlike the already experimental studies, the study presents a comprehensive and simultaneous physiochemical understanding (impact of ions, pH, surface charges, salinity, ionic strength, electrical conductivity, and dilution ratios) to elevate potential scale formation during low salinity water utilization to improve wettability alteration in sandstone oil reservoirs; (2) comprehensive and simultaneous investigation for determining the optimum dilution ratio, salinity, LSW composition according to minimum scale-risk; (3) this study illustrated that SW#10D with optimum salinity, dilution, and ionic composition was prepared for low salinity water injection, which could improve wettability alteration to water-wet state. However, increasing and reducing dilution times of SW#10D can enhance the risk of scale precipitation and increase cost and operation at the field scale. As a result, OLSW (SW#10D) is characterized by the control potential for scale deposition and more capacity for wettability alteration at the same time. In the final, this work presents the result of a comprehensive examination involving the developed LSW with an optimum concentration as a new promising technique for EOR that could be more efficient and cost-effective for successful wettability alteration and formation damage in minimum scale deposition.

Prediction of scale formation in oilfields

One of the significant challenges facing oil industry is predicting mineral scale formation because of several factors such as supersaturation, changes in the thermodynamic condition, ionic strength, pH, alkalinity, and flow velocity^{36,46}. There are many different solubility prediction methods for inorganic scales in oil and gas wells and reservoirs. Thermodynamic models are the most effective method that can be applied to inhabit and control mineral scale formation in wells and reservoirs. Because these models included the interference and effect of important thermodynamic factors such as temperature and pressure. According to the solubility limitations, available thermodynamic models can only predict the scale deposition's potential^{47,48}. The supersaturation of the aqueous solution can contribute to the nucleation and growth of the scales, as demonstrated by the saturation index (SI) and the saturation ratio (SR)^{33,36,39}.

Prediction of saturation index (SI). To evaluate of water compatibility between the LSW and formation brine, SI is regard a measurable parameter to determination the scale deposition⁴⁹. SI is expressed as scale precipitation of brine ratio to scale deposition, and the logarithm of ion concentration products must be divided by an equilibrium constant. For each scale, SI is defined as follows^{36,50,51}:

$$SI = \left(\frac{\text{ion activity product}}{K_{sp}(P,T,I)} \right) \quad (1)$$

Or

$$SI = \log(SR) = \log \frac{[Me] \times [An]}{K_{sp(P,T,I)}} = \log([Me] \times [An]) - \log K_{sp(P,T,I)} \quad (2)$$

Hence, based on the ionic activity coefficient, Eq. (5) can be written as the following formula³⁶:

$$SI = \log(SR) = \log_{10} \left\{ \frac{\alpha_{Me} \times \alpha_{An}}{K_{sp(P,T,I)}} \right\} = \log\{\alpha_{Me} \times \alpha_{An}\} - \log K_{sp(P,T,I)} \quad (3)$$

While in these equations [Me] include cations of Mg^{2+} , Ca^{2+} , Sr^{2+} , and Ba^{2+} , [An] includes anions or negative ions such as HCO_3^- and SO_4^{2-} , and K_{sp} denotes the solubility product of aqueous solution under reaction situation. If the saturation index equals 0 ($SI = 0$), then a liquid medium is saturated. In addition, when the saturation index has lower values than zero ($SI < 0$), the undersaturated situation and scale will not precipitate⁵². Ultimately, when the SI has greater values than 0 ($SI > 0$), it indicates that an aqueous solution is supersaturated and mineral scale tends to form^{35,36,47,53,54}. The SI values for an aqueous solution under different conditions are shown in Table 1^{36,55}.

Materials and methods

One critical parameter to study the deposition–precipitation mechanism is the composition of formation and injection brines to elevate scale formation phenomena and the mixing ratios of two brines. This study was conducted on low salinity water obtained from the Persian Gulf (seawater) for feasibility as injection water and formation damage created as mineral scale formation. For the investigation of the value and type of scales, the compatibility brine tests of mixing low salinity water compositions with formation water were performed at different ratios of 20%, 40%, 50%, 60%, and 80% and reservoir temperature ($T = 65^\circ C$). As a result, the maximum scale precipitation ratio was obtained to concern mineral scale formation. In the second stage, The FESEM-EDX tests were conducted on filters samples after compatibility tests for determination of scale types. In the third stage, The FESEM image and contact angle test were conducted to evaluate the wettability alteration. In the last stage, the lab tests were carried out on sandstone rock powder for the Z_p evolution and effect surface charges on scale deposition and wettability alteration in line with the FESEM and contact angle findings.

Materials. *Brines.* In the first step, formation and injection brines were synthesized, whereas formation water had the same composition as the reservoir brine, and Persian Gulf water (PGW) (seawater that is nearby to the sandstone field from southwest Iran) was chosen as a suitable supply for injection water. All samples of the brine compositions were synthesized in the lab that could dissolve in the given quantity of six salts at high purity from Merck Chemicals (purity of 99.5%), including NaCl, KCl, Na_2SO_4 , $NaHCO_3$, $MgCl \cdot 6H_2O$, and $CaCl_2 \cdot 2H_2O$ dissolved in deionized water. deionized water as 3-time evaporation distilled water with a resistivity of 18.2 M Ω cm was utilized. Table 2 shows the compositions of the formation and injection brines (seawater) used in this study. The formation water composition belongs to one of the oil reservoirs in southwest Iran. Also, the water composition of the Persian Gulf was used as injection water (seawater). The total dissolved solids (TDS) were 195,671.03 and 40,687 ppm for FW and SW, respectively. It should be mentioned that formation water had high-level salinity, total dissolved solids (TDS), total suspended solids (TSS), and different anions and cations in solution³¹. Various concentration levels of the injection water were prepared based on seawater collected from the Persian Gulf composition.

Crude oil. The crude oil from one of the Iranian southwestern reservoirs was applied in this work. The chemical composition and physical properties of the crude oil is presented in Tables 3 and 4. Also, Table 3 states that the value of C_1 is equal to 45.59% and C_{7+} is equal to 30.24%.

Stearic acid and n-heptane chemicals. A concentration of 0.01 molar of stearic acid solution in n- heptane was applied to wettability alteration the rock samples. The n-heptane and stearic acid were purchased from Merck.

Sandstone rock sample. In this study, in the first stage, several sandstone rock outcrops were needed for zeta potential and contact angle experiments. For these experiments, the rock powders and thin slices were prepared from the sandstone rock slabs. It should be mentioned that the rock slabs were not aged in formation brine first. Also, to obtain rock powder with uniform particle size and appropriate range for measuring zeta potential, the sandstone outcrops were crushed and passed through 2 sieves with consecutive meshes (mesh numbers 325 and 400). The particle size distribution in the lower sieve is in the range of 37–44 microns⁵. X-ray diffraction

SI	Description
SI = 0	An aqueous solution is saturated, indicating that the scale has no tendency for the formation or dissolution
SI < 0	An aqueous solution is undersaturated, suggesting that scale has no tendency for dissolution
SI > 0	An aqueous solution is supersaturated; resulting scale has tendency for formation

Table 1. Interpretation of saturation index.

Ions	Unit	Formation water	Seawater (Persian Gulf)
Na ⁺	mg/l	59,142.47	126.53
K ⁺	mg/l	0	420
Ca ²⁺	mg/l	135,00	498
Mg ²⁺	mg/l	1,725	1408
SO ₄ ²⁻	mg/l	449	3037
Cl ⁻	mg/l	120,444.44	22,598
HCO ₃ ⁻	mg/l	293	73
TDS	mg/l	195,671.03	40,687
Density	g/ml	1.126	1.02
Total alkalinity	mg/l as HCO ₃	293.06	73
Salinity	mg/l as NaCl	198,131.10	37,173.71
pH	-	6.5	8.13
EC	ms/cm at 25 °C	130	58
Ionic strength	Molal	1.73	0.829

Table 2. Complete water compositions of the formation water and seawater.

Components	C ₁	C ₂	C ₃	iC ₄	nC ₄	iC ₅	nC ₅	C ₆	C ₇	C ₈	C ₉	C ₁₀	C ₁₁	C ₁₂ ⁺	H ₂ S	CO ₂
Reservoir Oil (mol%)	45.59	7.02	4.28	0.87	2.13	0.88	0.88	4.78	1.33	3.14	1.72	2.04	1.78	23.21	0	0.21

Table 3. Crude oil properties.

M.W (g/mol)	Sp.gr	API	Viscosity (cp)
86	0.64	32.24	0.41

Table 4. The physical properties of crude oil.

fluorescence (XRF) analysis was used to evaluate the lithology of the core because the lithology of rock showed an effective impact on zeta potential measurement. The results obtained from the XRF analysis show that the mineralogy of the rock outcrop presented in Table 5. The abbreviation of LOE stands loss on ignition in Table 5.

Methods. *Brine compatibility studies and determining the most optimal injection water for preparation and making low salinity water.* In addition to the thermodynamic OLI ScaleChem software according to temperature, pressure, and pH changes, also laboratory experiments were performed to judge the compatibility/incompatibility of formation and injection waters to determine the mass and types of scale precipitation. Laboratory compatibility tests were conducted to determine the scale precipitation of mixing formation water with injection water and selecting the best injection water for the preparation of the optimum concentration of low salinity water. A schematic diagram of compatibility tests and determination of the type and amount scales is shown in Fig. 2. Compatibility tests were performed at atmospheric pressure. To assess the impact of the salinity of the injection water on the mineral scale deposition, injection waters with different types of salinity including without dilute, 2 (SW#2D), 5 (SW#5D), 10 (SW#10D), 15 (SW#15D), 20 (SW#15D) and 25 (SW#25 D) times diluted seawater (SW) were synthesized. Table 6 shows the compositions used to make up injection brines for the initial compatibility test and determine the optimal injection brine with the lowest mineral scale deposition. Ultimately, low salinity waters were prepared based on this optimal water composition. Afterward, injection water samples (including SW, SW#2D, SW#5D, SW#10D, SW#15D, SW#20D, and SW#25D) were mixed with formation brine at different mixing ratios of 20%, 40%, 50%, 60%, and 80%. To perform each compatibility test, 50 cm³ of each injection brine was filtered, poured into an autoclavable bottle, and mixed with 50 cm³ of formation water. The autoclavable bottles were placed in an oven at atmospheric pressure and reservoir temperature (65 °C) for 3 days for the effective reaction between ions. Also, these mixed waters were shaken twice in the morning and evening. The main cause of scale formation is the supersaturation of a solution of one or more salts in the aqueous

Element	SiO ₂	Al ₂ O ₃	BaO	CaO	Fe ₂ O ₃	K ₂ O	MgO	MnO	Na ₂ O	P ₂ O ₅	SO ₃	TiO ₂	LOI
Value (%)	36.59	2.14	<	29.54	1.65	0.45	2.22	>	0.33	0.08	0.09	0.13	26.79

Table 5. The results of XRF analysis of core samples.

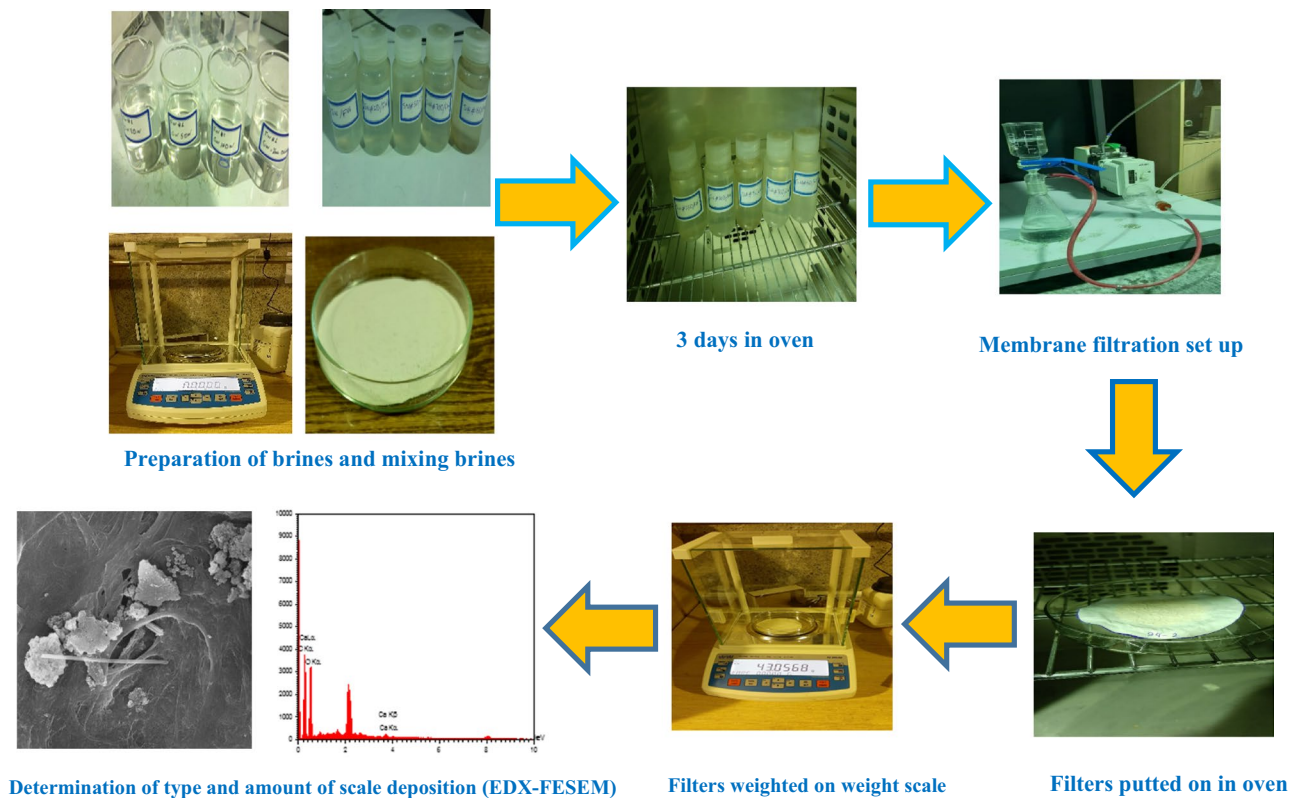


Figure 2. A schematic diagram of compatibility tests and determination of the type and amount scales.

Ions	Unit	Seawater (PG)	SW#2D	SW#5D	SW#10D	SW#15D	SW#20D	SW#25D
Na ⁺	mg/l	126,53	6326.50	2530.60	1265.30	843.53	632.65	50.52
K ⁺	mg/l	420	210	84	42	28	21	16.8
Ca ²⁺	mg/l	498	249	99.60	49.80	33.20	24.90	19.92
Mg ²⁺	mg/l	1408	704	281.6	140.8	93.87	70.4	56.32
SO ₄ ²⁻	mg/l	3037	1518.50	607.40	303.70	202.47	151.85	121.48
Cl ⁻	mg/l	22,598	11,299	4519.6	2259.8	1506.30	1129.90	903.92
HCO ₃ ⁻	mg/l	73	36.50	14.60	7.30	4.87	3.65	2.92
TDS	mg/l	40,687	20,343.50	8137.40	4068.70	2712.47	2034.35	1627.48
Salinity	mg/l as NaCl	37,173.71	18,586.85	7434.74	3717.37	2478.24	1858.68	1486.94
pH	–	8.138	8.13	8.13	8.13	8.13	8.13	8.13
EC	ms/cm at 25 °C	58	29	11.60	5.80	3.87	2.90	2.30

Table 6. Different low-salinity water compositions of Persian Gulf seawater with types of dilution.

phase^{36,52,56}. After 72 h, all samples were passed through a 0.22 μm membrane filter, and then the mass of scales on the membrane filter was calculated by an electronic top pan balance. In addition, the filters were exposed to deionized water by filtering deionized water to remove the residual NaCl (halite) salt, which probably covered the scale's surface because NaCl salt was a soluble salt in water and its deposit was unimportant.

Wettability alteration process. According to liter review^{57–64}, fatty acids could change the surface rock wettability from water-wet to oil-wet. As the surface of sandstone rocks was usually water-wet due to chemical structure, the initial wettability of rocks was altered toward oil-wet for the test, using a stearic acid/n-heptane mixture. Stearic acid is a fatty acid with a chemical formula of CH₃(CH₂)₁₆COOH and a molecular mass of 284.48 g/mol and is soluble in normal heptane and heavier alkanes. Normal heptane at ambient temperature has viscosity and density of 0.879 cp and 0.73 g/cm³, respectively. The sandstone rock samples were oil wetted by 0.01 molarity of stearic acid/n-heptane liquid at 65 °C for 4 days. Figure 3 shows the wettability alteration situation of thin slices before and after the aging process. The contact angle experiment (Fig. 3B) proved the wettability shift toward oil wetness.



Figure 3. Images of contact angle change of an oil droplet on the sandstone surface solutions before (A) and after (B) wettability alteration aged by 0.01 M stearic acid and n-Heptane.

Field emission scanning electron microscopy/energy dispersive X-ray spectrometry (FESEM/EDX). In this study, FESEM-EDX was performed on the post-treatment filters to examine the potential scale deposition after the interaction of different injection brines with the formation brine. FESEM images could help to determine the local scaling behavior and surface modification effect of the treatment brines. In addition, EDX results were applied for the local elemental analysis and chemical characterization of the post-treatment filter surface. Also, FESEM images were interpreted utilizing the results from the contact-angle measurement subsection, which could provide a qualitative investigation of the wetting aspects of the rock surfaces. The surface morphology of filters was investigated with FESEM images utilizing Tescan MIRA3 FEG (Czech Republic) with an acceleration voltage of 20 kV. In addition, Tescan MIRA3 was used for EDX analysis to identify the number of atoms filled on the surface of filter samples.

Apparatus for measuring the zeta potentials. Zeta potential (Z_p) can measure the injected water samples based on EOR performance⁶⁵. Z_p presents the value of the surface charge of the particles in a colloidal solution. Electrophoresis is defined the move of a charged particle proportion to the solution that is suspended under the effect of a utilized electric field⁶⁶. The electrophoretic mobility of suspended sandstone particles and brine was measured by the apparatus, after the Z_p value was determined. The Z_p of colloidal dispersions was measured using laser Doppler electrophoresis (LDE). In the LDE, a voltage across a cell is used, and the electrophoretic mobility of particles is obtained from the frequency shift observed in the scattered light^{67,68}. The electrophoretic mobility measure is the best and simplest manner to estimate the Z_p ⁶⁹. Finally, Z_p is dependent on electrophoretic mobility and calculated using the Henry equation as follows^{66,70}:

$$U_E = \frac{2\varepsilon z F(k a)}{3\eta}, \quad (4)$$

where, U_E is electrophoretic mobility, z is zeta potential, ε is dielectric constant, $F(ka)$ is Henry's Function, and η is viscosity. The changing composition of injection brines and diluted seawater levels also change the surface charge of the surface rock. The changes in surface charges show a good sign of injection brine success to wettability modification of surface rock toward water-wet³⁹. The surface charge of solutions was measured by applying the Malvern Zetasizer Nano ZS apparatus for oil-wet sandstone particles scattered in the desired aqueous solution. The amount of surface charge was reported as the Z_p of different brine samples. As above mentioned, the rock powders were aged in n-Heptane and 0.01 M stearic acid at 65 °C and 101.3 kPa pressure until rock powders became oil-wet. The aged sandstone particles scattered in the water sample were prepared by mixing 0.5 g of powdered sandstone particles with 50 cm³ of brine, representing by weight 1% of an aqueous suspension⁴⁵. The solutions were sonicated for 20 min using a sonication tool and held for 48 h to reach the equilibrium conditions. An agreeable Z_p amount was chosen about the mean amount from each sample.

Results and discussion

Identification and determination of scales using commercial OLI ScaleChem software. As previously mentioned, the most important factor on scale formation in an aqueous solution is the supersaturation condition. This condition occurs when the concentration of dissolved salts in an aqueous solution is higher than a saturated solution^{12,36,52}. Therefore, a supersaturation situation leads to precipitation, deposition, and the crystal growth of carbonate scales. For each mix of two incompatible waters (one including the excessive values of bicarbonate ions and the other including the excessive values of calcium ions), the Scaling Tendency (ST) is defined as the ratio of the ion activity product (IAP) divided by the equilibrium constant (K_{sp}). Consequently, it is the stimulation force for the precipitation reaction³⁶. A greater degree of supersaturation can result in a greater possibility for CaCO₃ precipitation. Mixing seawater (including high bicarbonate ions) with formation brine (including high calcium ions) led to calcium carbonate precipitation. Before performing laboratory tests designed to study the compatibility of brine, the OLI Scale software was applied to predict the potential of mineral scale precipitation due to mixing the injected seawater and low-salinity brines with formation water (see brine composition analysis data in Tables 2 and 6)⁷¹. It could help us describe different types of mineral scales formed in the aqueous solutions after mixing different low salinity brines with FW³⁵. In addition, the simulation can determine the mixing ratio that the potential of scale formation occurs at the highest value. The injection brines and FW's chemical ionic composition were used in the mixed brine simulation model to estimate mass precipitation rates and the types of scales. The prediction of CaCO₃ and CaSO₄ scale tendencies because of mixing the injected seawater with formation water is presented in Figs. 4 and 5, respectively. The maximum

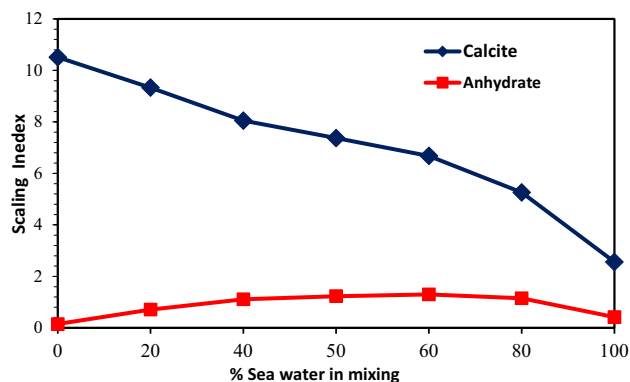


Figure 4. The scaling index of CaCO_3 and CaSO_4 scales at different mixing ratios of injection water (seawater) and formation water.

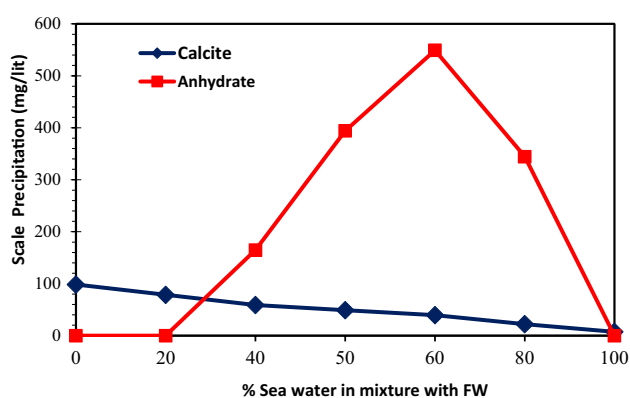


Figure 5. The amount of scale precipitation of CaCO_3 and CaSO_4 scales at different mixing ratios of injection water (seawater) and formation water.

precipitation was 549.18 mg/L for CaSO_4 at 60% seawater and 78.65 mg/L for CaCO_3 at 20% seawater. The ionic activity and the solubility are important factors on scale deposition¹². Therefore, the reason of maximum scale formation at mixing ratio of 60% was that by increasing the mixing ratio of seawater to 60%, the concentration of bicarbonate, calcium, and sulfate ions increased to the same ratio. Consequently, in this condition, both the ionic activity and the solubility increased. In other words, by increasing the percentage of seawater in mixing brine up to 60% that the interaction between anions and cations was increased and the solubility of mineral scales in brine was reduced. Therefore, there was a maximum mixing ratio in which the maximum amount of scale cannot dissolve in solution and the supersaturation conditions increased. However, after this mixing ratio, as the mixing ratio became more increased, the activity of calcium and sulfate ions decreased, and the solubility of mineral scales in brine increased¹². As a result, due to the reduction of supersaturation conditions, the amount of total scale deposition decreased. After changing the composition of seawater as low salinity water at different diluted seawater levels, the value of CaSO_4 precipitation was insignificant compared with that of CaCO_3 as the increasing dilution and reduction of the salinity seawater.

To obtain more accurate results, the impact of salinity on scale precipitation and the impact of the salinity of the injection SW on the value of CaCO_3 precipitation were investigated. Accordingly, optimum composition and salinity with increasing dilution and different salinities of injected SW were determined. Thus, the mixing proportion of seawater and formation brine showed no effect on the outcomes. The 50% mixing proportion of low salinity water with a different degree of dilution mixed with formation brine was chosen to conduct the compatibility tests.

The effect of salinity and dilution time of SW at different mixing ratios on the scale deposition. The CaCO_3 mineral scale tendency and scale deposition result in various mixing ratios of seawater and low salinity water in different diluted seawater levels and formation brine are presented in Figs. 6, 7 and 8, respectively. Tables 2 and 6 shown that some Ca^{2+} and HCO_3^- ions were observed in both formation brine and injected low salinity water can be formed CaCO_3 scale. The value of the mineral scale was estimated using the OLI ScaleChem and outlined in Fig. 6 for various dilutions and salinities of SW at different mixing ratios of SW/FW. Figure 7 shows the distribution of saturation ratio magnitude contours. Figures 6 and 7 shown that the amount of the CaCO_3 scale tendency was higher than 1; therefore, the CaCO_3 scale was formed at different

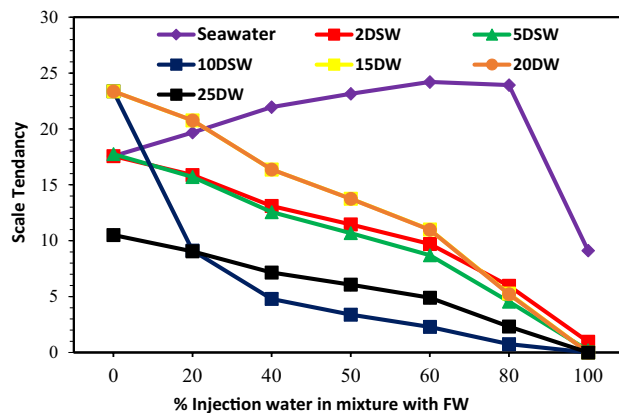


Figure 6. CaCO₃ (Calcite) scale tendency at reservoir conditions.

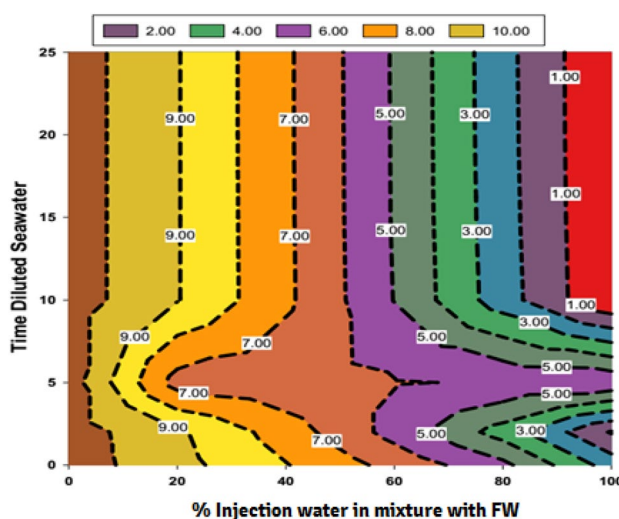


Figure 7. Counter plot of saturation ratio (SR) for diluted seawater ratios versus mixing ratios.

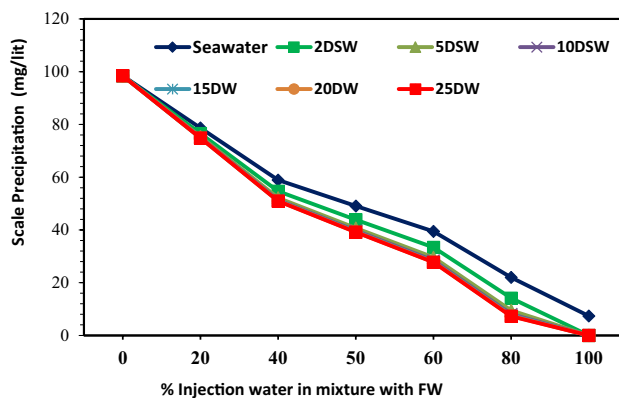


Figure 8. CaCO₃ scale precipitation at reservoir conditions.

mixing ratios of SW and FW. As depicted in Figs. 6, 7 and 8, by increasing the mixing ratio from the injected waters to the oil reservoir, the amount of CaCO₃ precipitation decreased. Also, as seawater's salinity decreased and dilutions increased, the ST and scale precipitation decreased due to calcium carbonate. Figures 6, 7, 8, 9 and 10 depict that the ST of 10-time diluted seawater (SW#10D) has a more noticeable decrease than other injected smart water, and its curve shows a greater decreasing trend. According to Fig. 7, the amount of scale deposition

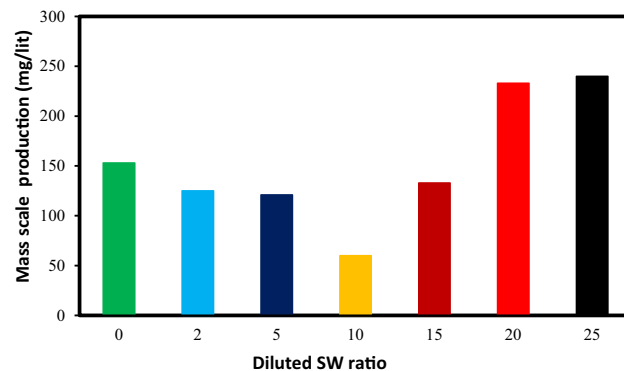


Figure 9. The amount of scale precipitation of mixing the diluted seawater with formation water (FW: SW # 0, 2, 5, 10, 15, 20, and 25 D).

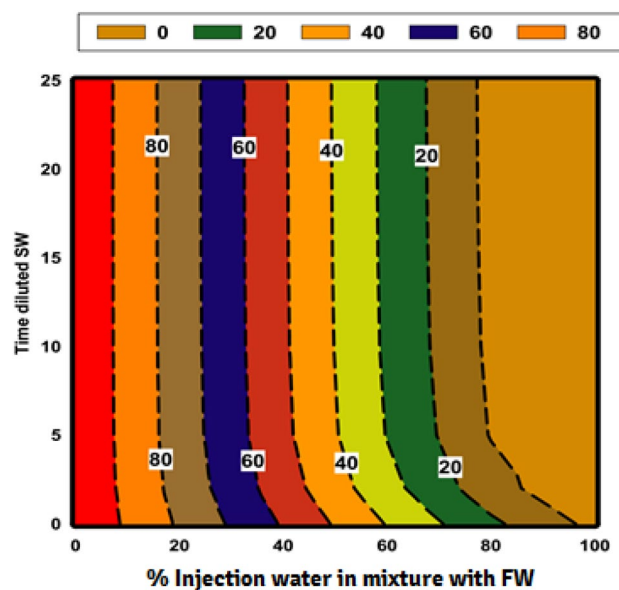


Figure 10. Scale deposition counters for different mixing ratios and different injection low salinity brines.

after 10-time diluted seawater (SW#10D) does not much change with increasing dilution to 15, 20, and 25 times. According to this figure, increasing dilution more than 10 times is not reasonable and cost-effective on a field scale in terms of cost and injecting a large volume of diluted injection water into the oil reservoir. Therefore, the optimal low-salinity injection water was 10 times diluted seawater. The laboratory results obtained from the compatibility test in a mixing ratio of 50:50 percent of SW/FW show that the lowest mineral scale formation rate occurred in 10 times diluted seawater. Figure 9 shows the amount of scale deposition of SW/FW in possibility and the actual situation in porous media of oil reservoir as mixing ratio of 50:50 percent of both brines. According to the compatibility test results and Fig. 8, the 10 times diluted SW (SW#10D) of Persian Gulf seawater composition has the highest solubility of salts and the least amount of mineral scale precipitation with the mixing of formation water. Therefore, the low-salinity water composition was the optimal composition of injected water into the reservoir. Also, the compatibility test results were consistent with the software simulation results. The scale amount in brine is related to total salinity (TDS) and reactive ion concentrations¹². Prior to SW#10 composition (OLSW), the further dilution ratio, the concentration of reactive ions was reduced. Therefore, the ionic activity and the solubility product parameters reduce, and the salinity parameter is a prevailing factor over the reactive ion concentration, and finally the total mass scale precipitation reduces. After that, the further dilution times further than SW#10 composition (OLSW), the activity of reactive ions (Ca^{2+} and HCO_3^-) increases in spite of the reduction in salinity of the brine. This means that the active ion amounts prevails over the salinity parameter, and this causes rising the activity of Ca^{2+} and HCO_3^- ions and arrives to quicker reactivity rise between the anionic and cationic ions, and finally higher scale deposition can occur¹². At optimal salinity and brine composition of 10 time-diluted seawater (SW#10D), there was an equilibrium state between ions concentration, pH, electrical conductivity, ionic strength, and the amount of carbon dioxide solution in the water. After this optimum condition, due to the reduction in the ions' activity in the complex formation, the amount

of scale precipitation decreased, and the mineral scale was formed slowly or stopped. Therefore, increasing the dilution without considering the active ions and their activity cannot guarantee reducing scale deposition during low salinity water flooding under reservoir conditions. After completion of compatibility tests, SEM–EDX analysis was conducted on scales deposited on filters owing to the mixing of formation brine and different injection brines to detect the kind and configuration of different scales. Also, the precise diagnosis of scale species and elemental composition was presented via EDX⁴⁵. Table 7 shows EDX analysis of formation water. Also, Fig. 11 shows the EDX spectra for formation brine in Table 7. EDX analyses of formation brine are shown in Fig. 11 and Table 7 are proved that Ca, O and C, S atoms have created small amounts of sulfate carbonate scale, and the prevailing type of scale is calcite. Table 8 shows EDX analysis of the 50% mixing ratio of seawater and formation water. According to EDX analysis, small amounts of sulfate scale and carbonate scale can be formed and the prevailing type of scale is calcite (Table 8). The EDX spectra also proved the low amount of CaSO₄ in the 50% mixing ratio of injection water and FW. EDX of mixing brines are shown in Fig. 12 and Table 8 that Ca, O and C atoms have created the prevailing type of calcite scale. However, lower amounts of S atom along with Ca, C, and O in the mixing composition indicate that a small amount of calcium sulfate can be formed, which is removed over time by diluting seawater due to a decrease in SO₄²⁻ concentration. Figure 13A,B show a FESEM image with a zoom of 5000 times and the EDX spectra of 50% LSW and formation water, respectively. In addition, EDX analysis of this composition is proved amounts of calcium carbonate scale (Table 9). The EDX spectra also proved the low amount of CaCO₃ in the 50% mixing ratio of OLSW (SW#10D) and FW (see Fig. 13B). As can be seen in Fig. 13B, in 50% injected brine and formation water composition, atomic picks of Ca, C, and O atoms are greater, which illustrates the scale deposition of CaCO₃. The same findings can be deduced from Fig. 12 for other samples. FESEM-EDX of mixing brines are shown in Fig. 13 and Table 9 that divalent cation (Ca²⁺) had created the prevailing type of scale that is calcite.

Elt	W%	A%
C	10.27	19.26
O	32.85	46.23
Mg	1.03	0.95
Cl	25.49	16.19
Ca	28.11	15.79
S	2.25	1.58
Dominant scale	CaCO ₃ and CaSO ₄	

Table 7. EDX analysis of formation water.

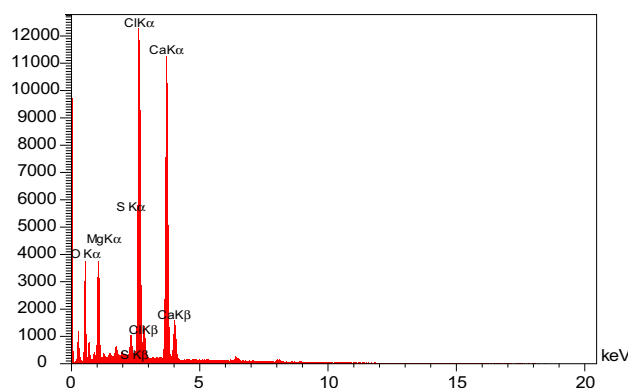


Figure 11. EDX analyses formation water of Table 7.

Elt	W%	A%
C	37.06	46.07
O	54.02	50.42
Ca	1.90	0.89
S	7.02	2.62
Dominant scale	CaCO ₃ and CaSO ₄	

Table 8. EDX analysis of mixing ratio 50% of formation water-seawater.

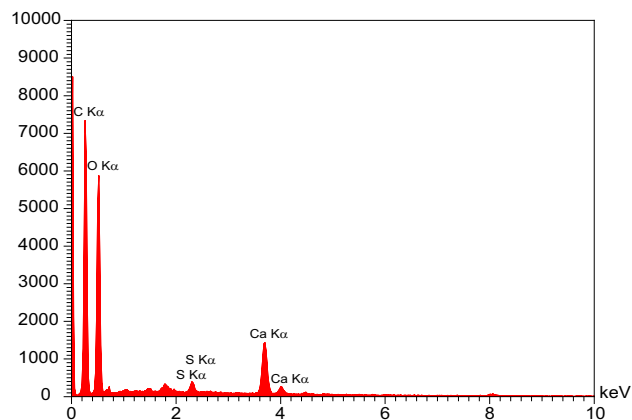


Figure 12. EDX analysis of seawater and formation brine composition at 50% mixing ratio of Table 8.

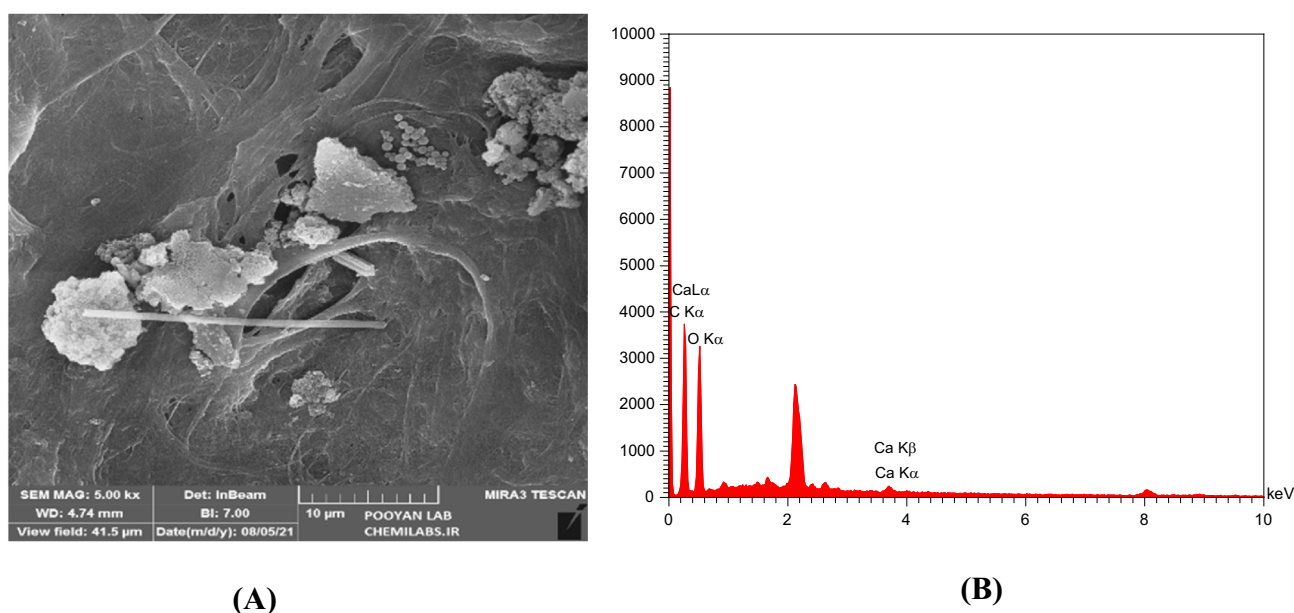


Figure 13. (A) FESEM image and (B) EDX analysis of mixing of LSW (SW#10D) and formation brine at 50% mixing ratio.

Elt	W%	A%
C	35.36	42.76
O	61.96	56.27
Ca	2.68	0.97
Dominant scale	CaCO ₃	

Table 9. EDX analysis of mixing ratio 50% of formation water-SW#10D in SEM image of Fig. 13.

Effect of concentrations of ions of injection brines at different mixing ratios and dilution ratios on CaCO₃ scale precipitation. Table 2 shows that the concentration of bicarbonate ion (HCO₃⁻) in seawater is very small (73 mg/L), whereas it is present in the formation water in large quantities (293 mg/L). Therefore, it can cause many problems due to the deposition of calcium carbonate in the production operating systems of this oil reservoir. Figure 14 shows Ca²⁺ ion concentration in different injection SW and low salinity waters versus different mixing ratios of SW/FW. The amount of calcium concentration has a declining trend with increasing dilution of seawater, and almost the amount of trend changes is constant with increasing mixing ratios. Also, the trend of Ca²⁺ concentration is almost within close range at different mixing ratios of SW/FW. The amount of Ca²⁺ ion concentration does not change by increasing the dilution of 10 times diluted seawater; therefore, these results correspond to the laboratory and simulation findings. The amount of HCO₃⁻ ions was decreased by

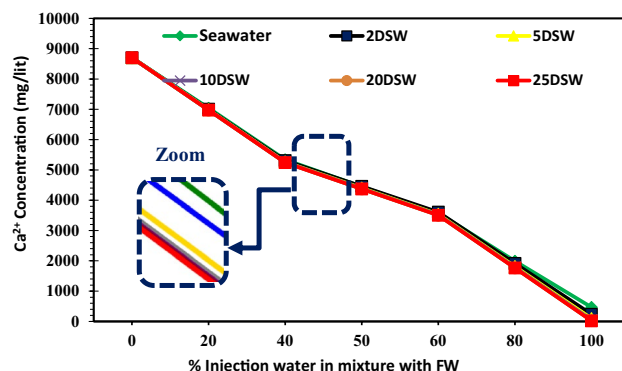


Figure 14. Variation of Ca^{2+} ion at different mixing ratios of injected water in diluted seawater level with the formation brine.

increasing mixing ratios and salinities (Fig. 15). As can be seen in Fig. 15, 10 times diluted seawater was an optimum concentration of bicarbonate ion; after this salinity, no change was observed in the trend of decline curve. In other words, the effect of optimal salinity is a complementary effect due to changes in calcium and bicarbonate ions, and the detection of optimum salinity can improve by changes in Mg^{2+} and HCO_3^- concentrations prior to Ca^{2+} concentrations. Reducing the concentration of bicarbonate ions to 10 times the initial amount in seawater, the amount of scale formed decreases (Fig. 15), and after this optimum LSW the amount of scale deposition does not change more. Therefore, diluting seawater more than 10 times is not economically suitable. Due to high charge density, Mg^{2+} ions are well covered at low temperatures by water molecules compared to Ca^{2+} ions. But, at high temperatures (above 70°C) due to dehydration, its activity increases. Therefore, Ca^{2+} ions' activity in the solution is overshadowed and reduces the reaction of SO_4^- ions with Ca^{2+} . As the solubility of calcium sulfate increases, less scale will be formed¹². Mg^{2+} ions can inhibit the rate of calcite nucleation. The concentration of the new nuclei is too dilute for each additional interference. The subsequent nuclei are then free of Mg^{2+} inhibition and have a normal growth rate, repressing the identity of reaction⁷². It can be expected that with increasing the concentration of magnesium ion, the amount of calcium carbonate precipitation corresponding to the rate of dilution ratio decreased (Fig. 16). However, the effect of Mg^{2+} ion has an intensity in low salinity brines. The addition of Mg^{2+} ions during calcium carbonate scale formation considerably affects the apparent solubility of the magnesium calcite phase formed. Therefore, effective scale inhibitors by magnesium ion may be due to active adsorption sites and a reduction in the thermodynamics of the formation of magnesium calcite scales⁷³.

Effect of pH and CO_2 concentration of SW at different salinities on scale formation. The mechanism of calcium carbonate scale formation with sulfate scales is different. This scale is mainly formed in oil reservoirs because of CO_2 emissions stemming from bicarbonate ions, resulting in a sudden decrease in pressure. The amount of CO_2 in the solution affects the pH of water and the solubility of CaCO_3 . At low pH values, the rate of calcium carbonate deposition is lower, and conversely, at high pH values, this amount is higher⁴⁷. When CO_2 is removed from the solution, the pH increases and the solubility of the soluble carbonates decreases, and most of the soluble bicarbonates become insoluble and also in the form of insoluble carbonates. Therefore, the solubility of bicarbonate ions at ambient pressure is very low. But, even this small amount can cause scale deposition

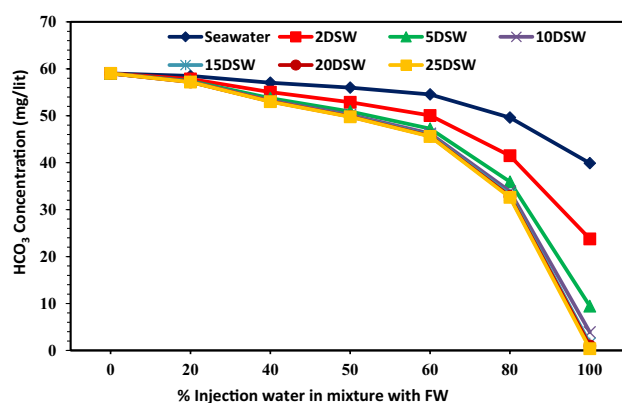


Figure 15. Variation of HCO_3^- ion at different mixing ratios of injection water in diluted seawater level with the formation brine.

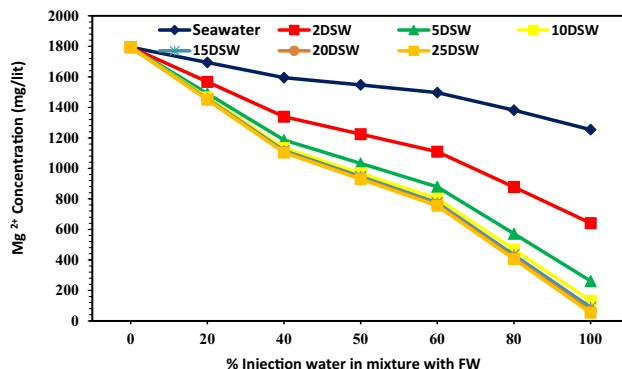


Figure 16. Variation of Mg²⁺ ion at different mixing ratios of injection water in diluted seawater level with the formation brine.

when mixing seawater with the formation water. So, in Fig. 18 is observed that with increasing the rate of water injection mixed with the formation water, the amount of dissolved carbon dioxide decreases. Also, it shows that the downward trend in the amount of carbon dioxide after 10 times diluting with water is almost constant. The results are fully compatible with the results of changes in bicarbonate ions in Fig. 15. Figure 17 shows pH changes with an increasing percentage of mixing of two brines. Therefore, with increasing the percentage of mixing of two brines, the pH increases. As previously mentioned, when CO₂ is released from the solution, the pH of the solution increases (Fig. 18).

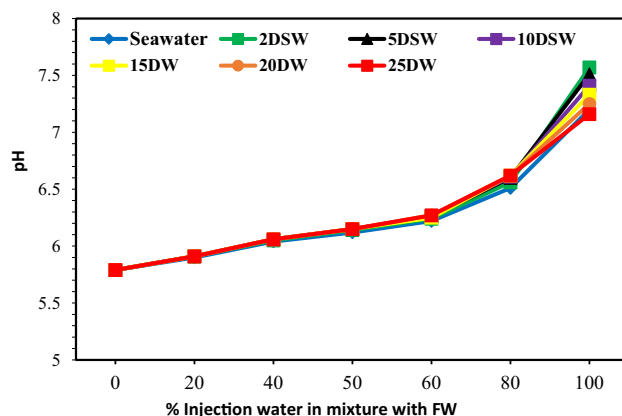


Figure 17. Variation of pH value at different mixing ratios of injection water in diluted seawater level with the formation brine.

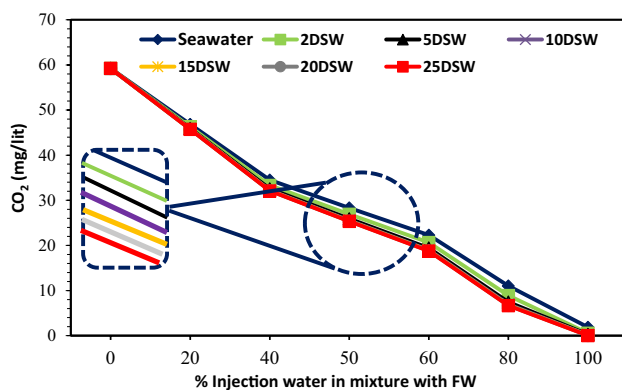


Figure 18. Variation of CO₂ concentration at different mixing ratios of injection water in diluted seawater level with the formation brine.

Effect of ionic strength and conductivity at different mixing ratios on CaCO₃ scale precipitation. The ionic strength (IS) of a solution depends on the concentration of ions amount of an aqueous solution. Therefore, the solution's ionic strength is considered a function of the concentration of total ions recognized in the solution. The IS of an aqueous solution can be defined as follows⁷⁴:

$$I = 1/2 \sum C_i Z_i^2. \quad (5)$$

C_i represents the concentration of ion i ($M = \text{mol/L}$); Z_i denotes the charge number of ions, and all ions in the solution are represented by the sum⁷⁴. The solubility product (K_{sp}) is also expressed in molality (m) concentrations and depends on both temperature and IS³⁶. The solubility of the CaCO₃ is highly influenced by the concentration of other ions observed in the system like Mg²⁺⁷². The solubility value of the CaSO₄ is higher than the SrSO₄, which in turn is nearly one and one-half orders of the amount higher than that of the BaSO₄⁷⁵. The variations of IS at different mixing ratios of injection brine of diluted seawater levels with formation brine are shown in Fig. 19; with increasing dilution times of seawater and decreasing SW salinity, IS decreased at different mixing ratios. After 10 times diluted seawater, the IS amount has not changed, and it is almost constant. In addition, according to Figs. 6, 7, 9, and 19, the ST of calcium carbonate was highly influenced by both the concentration of other ions observed in the system and the ionic strength. Then, as previously shown, after 10 times diluted seawater, the amount of activity ions' concentration at different mixing ratios of SW/FW was nearly constant. Therefore, it is expected that IS for other low salinity waters such as 15, 20, and 25 times diluted seawater has no change. One simple way to determine the concentration of suspended minerals in water is to measure EC. Distilled water or pure water is almost not a conductor of electricity. However, if salts are present in water, water can be a conductor of electricity. Therefore, the higher amount of salts dissolved in water, the higher EC; in other words, its electrical resistance decreases. The conductivity of water indicates ability of the electrification current to pass through the aqueous solutions. The electric current in solutions is guided by ions' motion, and the higher number of ions (the higher the concentration of soluble salts), the greater ionic mobility and the higher EC. Since EC is directly related to TDS and water-soluble salts, by measuring it, the amount of soluble solid particles and thus depositions of these in the solution can be measured by reducing the EC of solution⁷⁶. The solution's amount of conductivity shows a suitable method for evaluating scale deposition during mixing low salinity waters as the mixing of injection water with formation water at different ratios¹³. Results of conductivity values in Fig. 20 show a decreasing trend for all brines with an increasing mixing ratio of SW/FW. Also, similar results were obtained of scale tendency and scale deposition in Figs. 6, 7 and 8. The concentration trend of activity ions for CaCO₃ scale formation at different mixing ratios was in agreement with the results obtained from conductivity measurements of low salinity brine. The findings show an optimum composition of diluted seawater including minimum scale deposition. Reduction in seawater salinity and increasing time diluted seawater is not suitable and practicable of economically and operationally aspects at higher compositions of OLSW. Consequently, increasing the time diluted seawater without examining active ions and their activities cannot guarantee to decrease scale deposition in the low salinity water flooding.

FESEM analysis and contact angle measurements for determination of wettability alteration. The wettability of reservoir rock has an important effective on oil recovery due to impact on liquids permeability, interaction between oil droplets and rock surface, and sticking of oil droplets on rock surface⁷⁷. As mentioned previously before wettability alteration was one of the main mechanisms of enhance oil production by LSW and smart water flooding^{78,79}. Field emission scanning electron microscopy (FESEM) can be used as a method for surface modification and the wettability alteration of carbonate and sandstone surfaces from oil-wet to water-wet^{60,80-82}. The quality of changing the wettability of sandstone surface from water-wet to oil-wet, coating, and surface adsorption with optimum low salinity water (SW#10D) with minimum scale deposition was assessed using the FESEM. Figure 21 illustrates the FESEM images of surface sandstone rock before and after the

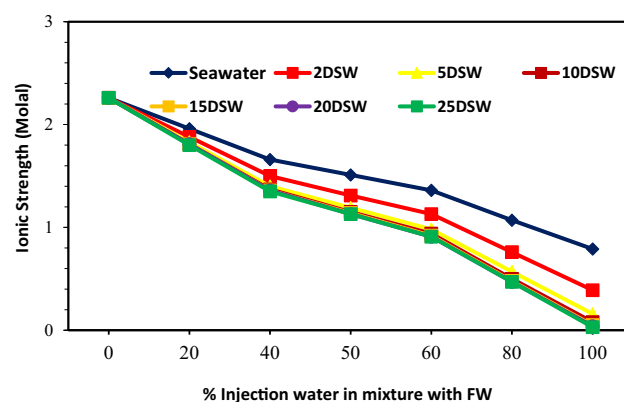


Figure 19. Variation of ionic strength at different mixing ratios of water injection in diluted seawater level with the formation brine.

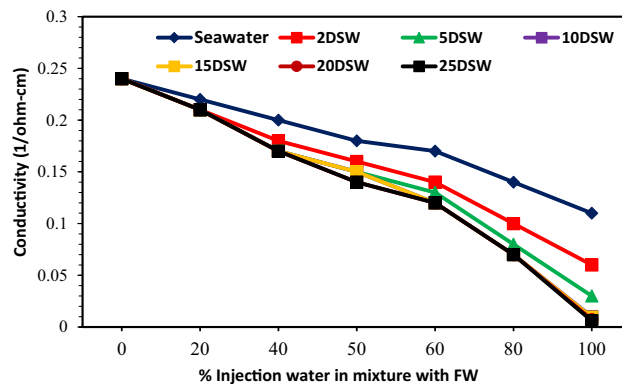


Figure 20. Variation of conductivity at different mixing ratios of water injection in diluted seawater level with the formation brine.

low salinity water treatments. Figure 21A,B shows the sandstone plate surface before aging (water wet) and after aging (oil-wet), respectively. The following figures show that the sandstone contains particles on a smooth surface (expected crystal edge). Then, the samples were aged by fatty acid (stearic acid) and n-heptane; the smooth surface was covered with a thin layer of oil, and its morphology was significantly modified (Fig. 21B). The sandstone surface had a gibbous hill without any smooth edge because of the adsorption of crude oil on its surface. The wettability of the sandstone plate surface could change from water-wet to oil-wet. The sandstone surface was aged in optimum low salinity water (SW#10D) for 24 h. Figure 21C shows the FESEM images of the sandstone rock surface after aging. It should be noted that in an oil-wet porous media, the impact of formation water on wettability alteration is less effective⁸³. The FESEM images show low salinity water well spear and adsorption on quartz surfaces. Mechanistically, negatively charged low salinity water composition can further alter the surface charge of quartz surface (Fig. 21). According to Fig. 21 and Zp results of Fig. 24, it can be concluded that the optimum low salinity water with minimum scaling alters the rock surface toward a negative charge. As a result, it could effectively modify the wettability of the sandstone surface to water-wet. Also, to rather study the effect of rock-OLSW interaction on ultimate oil recovery, the tendency and amount of wettability change should be examined. Therefore, a contact angle test was carried out at optimum low salinity water (SW#10D) with regard to time. Figure 22 shows the contact angle of optimum low salinity water (SW#10D)/crude oil/sandstone rock system with time, for 5 days to reach equilibrium. The contact angle measurements shown that contact angle in presence of OLSW reduced to 50.13° after 5 days. Therefore, the contact angle outcomes display the wettability alteration toward water-wetness over time. As a result, FESEM and contact angle findings confirmed Zp results, it was mean that OLSW was able to make sandstone surface more negative with diluting seawater and wettability changed from oil-wet toward water-wet.

Impact of dilution, salinity and brine composition on rock surface charge and wettability alteration. The impact of LSW is ascribed to the change in wettability, which is chiefly due to the expansion of the electrical double layer (EDL)⁸⁴. An electrical field that adsorbs differently charged ions is created due to the charged surface being in touch with LSW; the ordered ions create a diffuse layer of charge beyond the charged surface (stern layer). Therefore, the EDL generated by the diffuse layer and the stern layer⁸⁵. Figure 23 shows a schematic diagram of the EDL in the brine/sandstone system. Therefore, when salinity reduces a thicker water film is created which causes expansion of the EDL by LSW brine, as a result, prepares a better possibility for oil sweep efficiency⁸⁴. An easy and fast way to investigate surface charge changes at OLSW/rock and OLSW/oil interfaces and expansion of the EDL is via measuring Zp values⁸⁶. The Zp value is a measurement of the electrical potential in the diffuse layer of the EDL⁸⁷. The Zp values were used to examine the surface charge changes of aged-rock powders separated by various brines, including seawater, different LSW compositions and OLSW (SW#10D) (see Fig. 24). As a result, the Zp measurements were conducted on brine/aged-rock powder and oil/brine suspensions to illustrate the impacts of dilution, ionic composition, and salinity on the EDL. Figure 24 displays the Zp values of the aged-sandstone rock powders dispersed in brines. The Zp values were the average of three measurements for the sample. Potential determining ions including Ca^{2+} , Mg^{2+} , and SO_4^{2-} can importantly influence the interactions at the LSW/rock interface that straight effects the EDL in oil reservoirs⁶⁸. These ions are attached to the rock surface and change the rock-brine interface charge⁸⁶. Therefore, the OLSW composition caused a more negative surface charge owing to ions adsorption on the surface rock. The negatively charged surfaces can be described by the adsorption of Ca^{2+} , Mg^{2+} , and SO_4^{2-} ions at the rock surface, and the CaSO_4^- and MgSO_4^- complexes can create on the sandstone surface⁶⁸. The negative surface charges on the OLSW/rock and OLSW/oil interfaces can yield electrostatic repulsion between the interfaces and donate to further positive disjoining pressure⁸⁸. On the other hand, the sandstone surface has some active sites for potential determining ions to attach and alter the charge at the rock-brine interface. Therefore, by changing the brine salinity, the competition of the ions for binding sites and their reaction with OH^- and H^+ ions in solution vary, which results in different zeta potential values also the rock surface charge can change⁸⁹. As the OLSW had an optimum salinity and ionic composition, surface charge values altered negatively. As a result, by reducing brine salinity and ionic

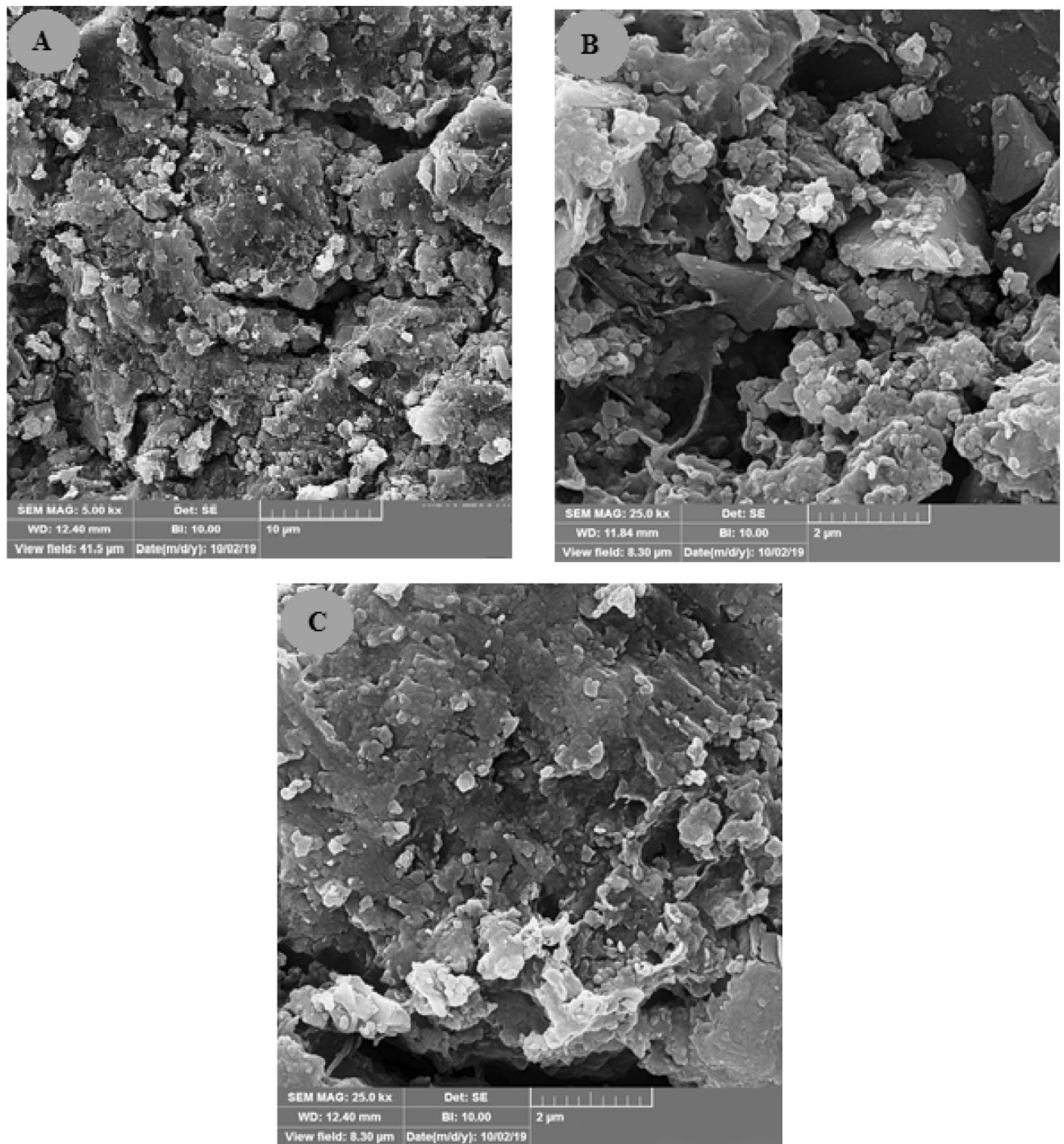


Figure 21. FESEM pictures of (A) a clean sandstone rock (water wet), (B) a sandstone rock aged in stearic acid and n-Heptane composition, and (C) an oil-wet sandstone rock aged in optimum SW#10D.

strength (FW > SW > SW#10D), the zeta potential presents more negative values (Fig. 24)⁸⁷. In addition, in a solution with higher salinity or lower conductivity the EDL evolves thinner. Therefore, the ions stack up on the EDL and forbid the liberation of potential determining ions³⁹. When OLSW is used as injection water due to changes at OLSW/rock and OLSW/oil interfaces, which decreases the adhesion force and attractive forces (or increase of repulsion forces) between the oil and rock surface and increases the expansion of EDL, resulting in the surface rock wettability changes to water-wet conditions^{84,90}. As a result, the optimum dilution and brine composition will yield the expansion of the EDL, which means a modification in the ionic brine composition. The findings are in good agreement with the contact angle measurement and FESEM findings.

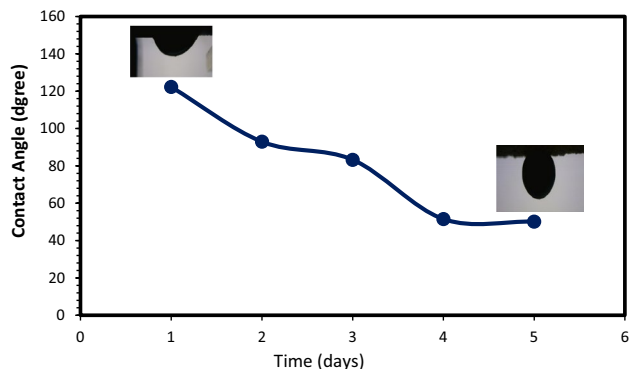


Figure 22. Contact angle variation of optimum low salinity water (SW#10D)/oil/sandstone rock with respect to time.

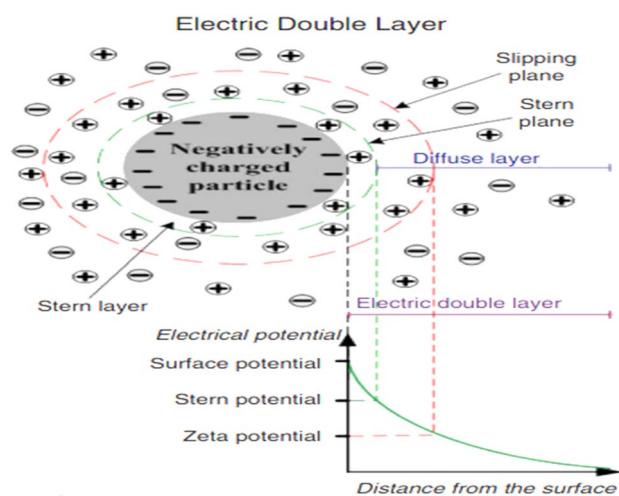


Figure 23. Schematic diagram of EDL in sandstone/brine system⁸⁴.

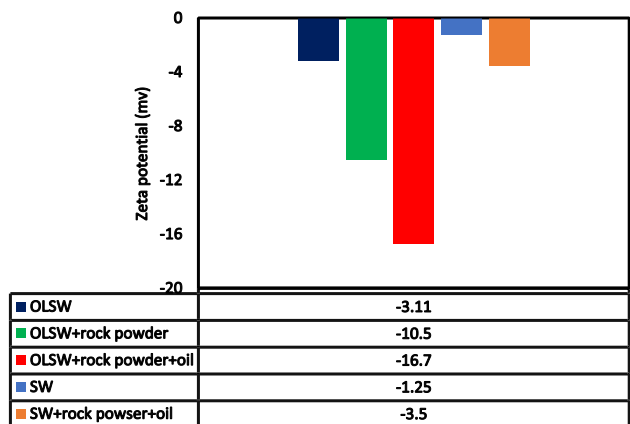


Figure 24. Zp values of aged sandstone rock powders scattered at different brines.

Conclusion

The principal results of this experimental study are summarized as following:

- The minimum amount scale can be formed in an optimal salinity and dilution and LSW composition (SW#10D). After this optimal amount, the ions concentration, electrical conductivity, ionic strength, pH, and scale precipitation amount do not significantly change and are almost constant. As a result, increasing dilution time at higher optimum SW#10 is not helpful from economic and operational points of view.
- A direct relationship was observed between salinity reduction, ion strength, electrical conductivity, effective ion concentrations (Ca^{2+} , Mg^{2+} , and HCO_3^-), and surface charge variations. The results showed that in an optimal salinity and dilution (SW#10D) and after this optimal amount, the values of these parameters did not significantly change.
- The simulation results and experimental tests (FESEM-EDX and compatibility test) confirmed that the CaCO_3 scale was the major scale when mixing injection water with formation water at different ratios. In addition, the CaCO_3 scale essentially showed a constant value in low salinity waters because it became increasingly dependent upon thermodynamic conditions when temperature and pressure were constant in different experimental conditions.
- In the optimum LSW composition (10DSW) the rock wettability changed from oil-wet toward water-wet conditions due to an increase in dilution ratio and reduction in salinity of injected water. Consequently, SW#10D is characterized by both the control potential for scale deposition and more capacity for wettability alteration at the same time.

Data availability

The datasets used and/or analyzed during the current study available from the corresponding author on reasonable request.

Received: 5 January 2023; Accepted: 3 August 2023

Published online: 10 August 2023

References

1. Singh Sidhu, H., Siddhamshetty, P. & Kwon, J. S. Approximate dynamic programming based control of proppant concentration in hydraulic fracturing. *Mathematics* **6**, 132 (2018).
2. Sen, D., Chen, H., Datta-Gupta, A., Kwon, J. & Mishra, S. Machine learning based rate optimization under geologic uncertainty. *J. Petrol. Sci. Eng.* **207**, 109116 (2021).
3. Abbasi, S. & Khamehchi, E. Investigation of permeability decline due to coupled precipitation/dissolution mechanism in carbonate rocks during low salinity co-water injection. *Energy Rep.* **7**, 125–135 (2021).
4. Alameri, W., Teklu, T. W., Graves, R. M., Kazemi, H. & AlSumaiti, A. M. In *SPE Asia Pacific Oil & Gas Conference and Exhibition*. (OnePetro).
5. Farhadi, H., Fatemi, M. & Ayatollahi, S. Experimental investigation on the dominating fluid-fluid and rock-fluid interactions during low salinity water flooding in water-wet and oil-wet calcites. *J. Petrol. Sci. Eng.* **204**, 108697 (2021).
6. Ali, J. A., Kolo, K., Manshad, A. K., Stephen, K. & Keshavarz, A. Modification of LoSal water performance in reducing interfacial tension using green ZnO/SiO₂ nanocomposite coated by xanthan. *Appl. Nanosci.* **9**, 397–409 (2019).
7. Raifei, A. & Khamehchi, E. Design of smart water composition based on scale minimization and its effect on wettability alteration in the presence of nanoparticles and mineral scales. *J. Petrol. Sci. Eng.* **196**, 107832 (2021).
8. Fasano, M. *et al.* Deep-sea reverse osmosis desalination for energy efficient low salinity enhanced oil recovery. *Appl. Energy* **304**, 117661 (2021).
9. Nasralla, R. A., Alotaibi, M. B. & Nasr-El-Din, H. A. In *SPE Western North American Region Meeting*. (OnePetro).
10. Wang, G., Chen, X., Liu, S., Wong, C. & Chu, S. Mechanical chameleon through dynamic real-time plasmonic tuning. *ACS Nano* **10**, 1788–1794 (2016).
11. Mahani, H. *et al.* Insights into the mechanism of wettability alteration by low-salinity flooding (LSF) in carbonates. *Energy Fuels* **29**, 1352–1367 (2015).
12. Ghasemian, J., Riahi, S., Ayatollahi, S. & Mokhtari, R. Effect of salinity and ion type on formation damage due to inorganic scale deposition and introducing optimum salinity. *J. Petrol. Sci. Eng.* **177**, 270–281 (2019).
13. Safari, M., Rahimi, A., Lah, R. M., Gholami, R. & Khur, W. S. Sustaining sulfate ions throughout smart water flooding by nanoparticle based scale inhibitors. *J. Mol. Liq.* **310**, 113250 (2020).
14. Nowrouzi, I., Manshad, A. K. & Mohammadi, A. H. Effects of dissolved binary ionic compounds and different densities of brine on interfacial tension (IFT), wettability alteration, and contact angle in smart water and carbonated smart water injection processes in carbonate oil reservoirs. *J. Mol. Liq.* **254**, 83–92 (2018).
15. Erke, S. *et al.* *SPE Improved Oil Recovery Conference* (Society of Petroleum Engineers).
16. Afekare, D. A. & Radonjic, M. From mineral surfaces and coreflood experiments to reservoir implementations: Comprehensive review of low-salinity water flooding (LSWF). *Energy Fuels* **31**, 13043–13062 (2017).
17. Ngo, I., Sasaki, K., Ma, L., Nguete, R. & Sugai, Y. Enhancing surfactant desorption through low salinity water post-flush during Enhanced Oil Recovery. *Oil Gas Sci. Technol. Revue d'IFP Energies nouvelles* **76**, 68 (2021).
18. Bijani, M., Khamehchi, E. & Shabani, M. Comprehensive experimental investigation of the effective parameters on stability of silica nanoparticles during low salinity water flooding with minimum scale deposition into sandstone reservoirs. *Sci. Rep.* **12**, 16472 (2022).
19. Nowrouzi, I., Manshad, A. K. & Mohammadi, A. H. Effects of Tragacanth Gum as a natural polymeric surfactant and soluble ions on chemical smart water injection into oil reservoirs. *J. Mol. Struct.* **1200**, 127078 (2020).
20. Abu-Al-Saud, M., Al-Ghamdi, A., Ayirala, S. & Al-Otaibi, M. In *E3S Web of Conferences*. 02003 (EDP Sciences).
21. Kataya, A., Khamehchi, E. & Bijani, M. The impact of salinity, alkalinity and nanoparticle concentration on zeta-potential of sand minerals and their implication on sand production. *Energy Geoscience* **3**, 314–322 (2022).
22. Alotaibi, M. B., Azmy, R. & Nasr-El-Din, H. A. In *SPE Improved Oil Recovery Symposium* (Society of Petroleum Engineers).
23. Yousef, A. A., Al-Saleh, S. & Al-Jawfi, M. S. In *SPE Middle East Oil and Gas Show and Conference* (Society of Petroleum Engineers).

24. Yousef, A. A., Al-Salehsalah, S. H. & Al-Jawfi, M. S. In *SPE EUROPEC/EAGE Annual Conference and Exhibition* (Society of Petroleum Engineers).
25. Aghaeifar, Z., Strand, S., Puntervold, T., Austad, T. & Sajjad, F. M. Smart Water injection strategies for optimized EOR in a high temperature offshore oil reservoir. *J. Petrol. Sci. Eng.* **165**, 743–751 (2018).
26. Fathi, S. J., Austad, T. & Strand, S. “Smart water” as a wettability modifier in chalk: The effect of salinity and ionic composition. *Energy Fuels* **24**, 2514–2519 (2010).
27. Wu, Y.-S. & Bai, B. In *SPE Reservoir Simulation Symposium* (Society of Petroleum Engineers).
28. Al Shalabi, E. W., Sepehrnoori, K. & Delshad, M. Mechanisms behind low salinity water injection in carbonate reservoirs. *Fuel* **121**, 11–19 (2014).
29. Korrani, A. K. N. *Mechanistic Modeling of Low Salinity Water Injection* (University of Texas, 2014).
30. Khormali, A., Petrakov, D. G., Lamidi, A.-L. B. & Rastegar, R. In *SPE European Formation Damage Conference and Exhibition* (OnePetro).
31. Cao, K., Siddhamshetty, P., Ahn, Y., El-Halwagi, M. M. & Kwon, J.S.-I. Evaluating the spatiotemporal variability of water recovery ratios of shale gas wells and their effects on shale gas development. *J. Clean. Prod.* **276**, 123171 (2020).
32. Garcia-Olvera, G. & Alvarado, V. In *SPE Improved Oil Recovery Conference* (OnePetro).
33. Abbasi, S. & Khamehchi, E. Experimental investigation of competitive mechanisms of precipitation and dissolution due to seawater and low salinity water injection in carbonate reservoirs. *J. Mol. Liq.* **324**, 114767 (2020).
34. Olajire, A. A. A review of oilfield scale management technology for oil and gas production. *J. Petrol. Sci. Eng.* **135**, 723–737 (2015).
35. Khormali, A., Petrakov, D. G. & Farmanzade, A. R. Prediction and inhibition of inorganic salt formation under static and dynamic conditions—effect of pressure, temperature, and mixing ratio. *Int. J. Technol.* **7**, 943–951 (2016).
36. Bijani, M. & Khamehchi, E. Optimization and treatment of wastewater of crude oil desalting unit and prediction of scale formation. *Environ. Sci. Pollut. Res.* **26**, 25621–25640 (2019).
37. Kumar, S., Naiya, T. K. & Kumar, T. Developments in oilfield scale handling towards green technology—A review. *J. Pet. Sci. Eng.* **169**, 428–444 (2018).
38. Khormali, A., Bahlakeh, G., Struchkov, I. & Kazemzadeh, Y. Increasing inhibition performance of simultaneous precipitation of calcium and strontium sulfate scales using a new inhibitor—Laboratory and field application. *J. Petrol. Sci. Eng.* **202**, 108589 (2021).
39. Abbasi, P., Abbasi, S. & Moghadasi, J. Experimental investigation of mixed-salt precipitation during smart water injection in the carbonate formation. *J. Mol. Liq.* **299**, 112131 (2020).
40. Abbasi, S. & Khamehchi, E. Experimental investigation of competitive mechanisms of precipitation and dissolution due to seawater and low salinity water injection in carbonate reservoirs. *J. Mol. Liq.* **324**, 114767 (2021).
41. Ezzati, S. & Khamehchi, E. Compatibility test and nanoparticles stability: Comparison between smart soft water and smart hard water. *SPE Prod. Oper.* (2020).
42. Moghadasi, R., Rostami, A., Tatar, A. & Hemmati-Sarapardeh, A. An experimental study of Nanosilica application in reducing calcium sulfate scale at high temperatures during high and low salinity water injection. *J. Petrol. Sci. Eng.* **179**, 7–18 (2019).
43. Tale, F. *et al.* Experimental and simulation study of low salinity brine interactions with carbonate rocks. *J. Petrol. Sci. Eng.* **184**, 106497 (2020).
44. Abbasi, S. & Khamehchi, E. Precipitation/dissolution and precipitants movement mechanisms effects on injectivity variations during diluted produced water re-injection into a layered reservoir—experimental investigation. *Energy Sources Part A Recovery Util. Environ. Eff.* **1–19** (2021).
45. Abbasi, P., Madani, M., Abbasi, S. & Moghadasi, J. Mixed salt precipitation and water evaporation during smart water alternative CO₂ injection in carbonate reservoirs. *J. Pet. Sci. Eng.* **208**, 109258 (2021).
46. MacAdam, J. & Parsons, S. A. Calcium carbonate scale formation and control. *Re/Views Environ. Sci. Bio/Technol.* **3**, 159–169 (2004).
47. Moghadasi, J., Jamialahmadi, M., Müller-Steinhagen, H. & Sharif, A. In *SPE International Symposium and Exhibition on Formation Damage Control* (Society of Petroleum Engineers).
48. Rocha, A., Frydman, M., Da Fontoura, S., Rosario, F. & Bezerra, M. In *International Symposium on Oilfield Scale* (Society of Petroleum Engineers).
49. Negahdari, Z., Khandoozi, S., Ghaedi, M. & Malayeri, M. R. Optimization of injection water composition during low salinity water flooding in carbonate rocks: A numerical simulation study. *J. Petrol. Sci. Eng.* **209**, 109847 (2022).
50. He, S., Kan, A., Tomson, M. & Oddo, J. In *SPE Annual Technical Conference and Exhibition* (Society of Petroleum Engineers).
51. Doubra, P., Kamran-Pirzaman, A., Mohammadi, A. H. & Hassanalizadeh, R. Thermodynamic modelling of scale (Calcite, Barite, Anhydrite and Gypsum) deposition from brine. *J. Mol. Liq.* **230**, 96–103 (2017).
52. Bijani, M., Behbahani, R. M. & Moghadasi, J. Predicting scale formation in wastewater disposal well of Rag-e-Safid desalting unit No. 1. *Desalin. Water Treat.* **65**, 117–124 (2017).
53. Oddo, J. & Tomson, M. Why scale forms in the oil field and methods to predict it. *SPE Prod. Facil.* **9**, 47–54 (1994).
54. Bellarby, J. *Well Completion Design*. Vol. 56 (Elsevier, 2009).
55. Ferguson, R. J. In *International Water Conference*. 77 (ESWP).
56. Hendraningrat, L. & Torsæter, O. Metal oxide-based nanoparticles: revealing their potential to enhance oil recovery in different wettability systems. *Appl. Nanosci.* **5**, 181–199 (2015).
57. Hansen, G., Hamouda, A. & Denoyel, R. The effect of pressure on contact angles and wettability in the mica/water/n-decane system and the calcite+ stearic acid/water/n-decane system. *Colloids Surf. A* **172**, 7–16 (2000).
58. Gomari, K. R. & Hamouda, A. Effect of fatty acids, water composition and pH on the wettability alteration of calcite surface. *J. Petrol. Sci. Eng.* **50**, 140–150 (2006).
59. Gomari, K. R., Denoyel, R. & Hamouda, A. Wettability of calcite and mica modified by different long-chain fatty acids (C18 acids). *J. Colloid Interface Sci.* **297**, 470–479 (2006).
60. Bahri, A. & Khamehchi, E. Investigating the effect of wettability on sand production in the presence of smart water and smart nanofluid: An experimental study. *Biointerface Res. Appl. Chem.* **10**, 6652–6668 (2021).
61. Montazeri, M. *et al.* An experimental investigation of smart-water wettability alteration in carbonate rocks—oil recovery and temperature effects. *Energy Sources Part A Recovery Util. Environ. Eff.* **1–13** (2020).
62. Jarraghan, K., Vafie-Sefti, M., Ayatollahi, S., Moghadam, F. & Moghadam, A. M. In *International Symposium of the Society of Core Analysts*. 4–7.
63. Bijani, M., Khamehchi, E. & Shabani, M. Comprehensive experimental investigation of the effective parameters on stability of silica nanoparticles during low salinity water flooding with minimum scale deposition into sandstone reservoirs. *Sci. Rep.* **12**, 1–19 (2022).
64. Hosseini-Kaldozakh, S. A., Khamehchi, E., Dabir, B., Alizadeh, A. & Mansouri, Z. Rock wettability effect on Colloidal Gas Aphron invasion near wellbore region. *J. Petrol. Sci. Eng.* **189**, 106766 (2020).
65. Bassioni, G. & Taha Taqvi, S. Wettability studies using zeta potential measurements. *J. Chem.* **2015**, 1–6 (2015).
66. Shaw, R. *Dynamic Light Scattering Training* (Malvern Instruments Ltd, 2014).
67. Derkani, M. H. *et al.* Mechanisms of surface charge modification of carbonates in aqueous electrolyte solutions. *Colloids Interfaces* **3**, 62 (2019).

68. Mehraban, M. F., Ayatollahi, S. & Sharifi, M. Role of divalent ions, temperature, and crude oil during water injection into dolomitic carbonate oil reservoirs. *Oil Gas Sci. Technol. Revue d'IFP Energies nouvelles* **74**, 36 (2019).
69. Dembek, M., Bocian, S. & Buszewski, B. Solvent influence on zeta potential of stationary phase—Mobile phase interface. *Molecules* **27**, 968 (2022).
70. Jarrahian, K., Seiedi, O., Sheykhan, M., Sefti, M. V. & Ayatollahi, S. Wettability alteration of carbonate rocks by surfactants: A mechanistic study. *Colloids Surf. A* **410**, 1–10 (2012).
71. OLI. OLI ScaleChem., ScaleChem. http://wiki.olisystems.com/wiki/OLI_Studio (2016).
72. Bischoff, J. L. Kinetics of calcite nucleation: Magnesium ion inhibition and ionic strength catalysis. *J. Geophys. Res.* **73**, 3315–3322 (1968).
73. Nancollas, G. & Sawada, K. Formation of scales of calcium carbonate polymorphs: The influence of magnesium ion and inhibitors. *J. Petrol. Technol.* **34**, 645–652 (1982).
74. Sheng, J. J. *Modern Chemical Enhanced Oil Recovery: Theory and Practice* (Gulf Professional Publishing, 2010).
75. Baraka-Lokmane, S. & Hurtevent, C. In *Abu Dhabi International Petroleum Conference and Exhibition* (OnePetro).
76. Duncan, D., Walker, M. & Harvey, F. *Regulatory Monitoring and Testing: Water and Wastewater Sampling* (Environment Protection Authority, 2007).
77. Yu, H. *et al.* Wettability enhancement of hydrophobic artificial sandstones by using the pulsed microwave plasma jet. *Colloid Interface Sci. Commun.* **36**, 100266 (2020).
78. Sharma, V. K., Singh, A. & Tiwari, P. An experimental study of pore-scale flow dynamics and heavy oil recovery using low saline water and chemical flooding. *Fuel* **334**, 126756 (2023).
79. Bijani, M., Khamehchi, E. & Ezzati, S. Silica nanoparticles and pH effect on sand production mechanism due to smart water softening. *Lett. Appl. NanoBioSci.* **9**, 1294–1306 (2020).
80. Aghajanzadeh, M. R., Ahmadi, P., Sharifi, M. & Riazi, M. Wettability alteration of oil-wet carbonate reservoir using silica-based nanofluid: An experimental approach.
81. Yang, J. *et al.* Wettability alteration during low-salinity waterflooding and the relevance of divalent ions in this process. *Energy Fuels* **30**, 72–79 (2016).
82. Dehghan Monfared, A., Ghazanfari, M. H., Jamialahmadi, M. & Helalizadeh, A. Potential application of silica nanoparticles for wettability alteration of oil-wet calcite: A mechanistic study. *Energy Fuels* **30**, 3947–3961 (2016).
83. Abedi, B., Castaño, E. P. M., Heidaryan, E. & Shadloo, M. S. Pore-Scale visualization on polymer flooding: application of singular value decomposition-based image analysis method. *J. Porous Media* **23** (2020).
84. Nasralla, R. A. & Nasr-El-Din, H. A. Double-layer expansion: Is it a primary mechanism of improved oil recovery by low-salinity waterflooding?. *SPE Reservoir Eval. Eng.* **17**, 49–59 (2014).
85. Farhadi, H., Ayatollahi, S. & Fatemi, M. Impact of rock morphology on the dominating enhanced oil recovery mechanisms by low salinity water flooding in carbonate rocks. *Fuel* **324**, 124769 (2022).
86. Mahani, H. *et al.* Insights into the impact of temperature on the wettability alteration by low salinity in carbonate rocks. *Energy Fuels* **31**, 7839–7853 (2017).
87. Jackson, M. D., Al-Mahrouqi, D. & Vinogradov, J. Zeta potential in oil-water-carbonate systems and its impact on oil recovery during controlled salinity water-flooding. *Sci. Rep.* **6**, 1–13 (2016).
88. Ebrahim, T., Mohsen, V. S., Mahdi, S. M., Esmaeel, K. T. & Saeb, A. Performance of low-salinity water flooding for enhanced oil recovery improved by SiO (2019).
89. Fazelnasab, M., Akhlaghi Amiri, H. A., Jalali, P. & Daliri, A. In *11th International Chemical Engineering Congress & Exhibition* (IChEC, 2020).
90. Mahani, H., Keya, A. L., Berg, S. & Nasralla, R. Electrokinetics of carbonate/brine interface in low-salinity waterflooding: Effect of brine salinity, composition, rock type, and pH on ζ -potential and a surface-complexation model. *SPE J.* **22**, 53–68 (2017).

Author contributions

M.B.: PhD in Petroleum engineering, conceptualization, methodology, laboratory tests, data analysis and visualization, writing original draft of manuscript. E.K.: Professor, Department of Petroleum Engineering supervision, reviewing and editing the manuscript. M.S.: Regional Technical Advisor at STRATUM Reservoir, Middle East, UAE, reviewing and editing the original draft of manuscript.

Competing interests

The authors declare no competing interests.

Additional information

Correspondence and requests for materials should be addressed to E.K.

Reprints and permissions information is available at www.nature.com/reprints.

Publisher's note Springer Nature remains neutral with regard to jurisdictional claims in published maps and institutional affiliations.



Open Access This article is licensed under a Creative Commons Attribution 4.0 International License, which permits use, sharing, adaptation, distribution and reproduction in any medium or format, as long as you give appropriate credit to the original author(s) and the source, provide a link to the Creative Commons licence, and indicate if changes were made. The images or other third party material in this article are included in the article's Creative Commons licence, unless indicated otherwise in a credit line to the material. If material is not included in the article's Creative Commons licence and your intended use is not permitted by statutory regulation or exceeds the permitted use, you will need to obtain permission directly from the copyright holder. To view a copy of this licence, visit <http://creativecommons.org/licenses/by/4.0/>.

© The Author(s) 2023